Steel and Composite Structures, *Vol. 34, No. 4* (*2020*) *581-597*
DOI: https://doi.org/10.12989/scs.2020.34.4.581

Structural lightweight concrete containing expanded poly-styrene beads; Engineering properties

Behnam Vakhshouri*

Faculty of Engineering and Information Technology, School of Civil and Environmental Engineering, University of Technology Sydney, Australia

(*Received April 27, 2019, Revised December 25, 2019, Accepted January 10, 2020*)

Abstract. Light-Weight Concrete containing Expanded Poly-Styrene Beads (EPS-LWC) is an approved structural and non-structural material characterized by a considerably lower density and higher structural efficiency, compared to concrete containing ordinary aggregates. The experimental campaign carried out in this project provides new information on the mechanical properties of structural EPS-LWC, with reference to the strength and tension (by splitting and in bending), the modulus of elasticity, the stress-strain curve in unconfined compression, the absorbed energy under compression and reinforcement-concrete bond. The properties measured at seven ages since casting, from 3 days to 91 days, in order to investigate their in-time evolution. Mathematical relationships are formulated as well, between the previous properties and time, since casting. The dependence of the compressive strength on the other mechanical properties of EPS-LWC is also described through an empirical relationship, which is shown to fit satisfactorily the experimental results.

Keywords: expanded polystyrene; lightweight concrete; Splitting tensile strength; flexural strength; compressive stress-strain curve; energy absorption; bond-slip; age factor

1. Introduction

The demand for structural Light-Weight Concrete (LWC) in modern construction applications such as high-rise buildings, offshore structures and long-span bridges is increasing. Reducing the weight of load-bearing elements by using lightweight concrete and enhancing the functionality of the structure are the main objectives in utilizing the LWC in construction industry. The reduced weight of structure brings in less energy demand during the construction, better steel-concrete bond, durability performance, tensile strain capacity and fatigue resistance (Tang 2017). The better insulation and thermal properties compared to Conventional Concrete (CC) are the other advantages of LWC in building construction (Tang 2015, Vakhshouri and Nejadi 2016).

Density and compressive strength are the main factors in the design codes to classify the LWC into the structural and non-structural concrete (Vakhshouri and Nejadi 2017). LWC can be obtained by introducing gas (or foam) into the paste or by wholly or partially replacing the standard aggregate with low-weight and preferentially low-cost components. The range of lightweight aggregates to produce LWC is wide, encompassing extremely light materials in non-structural concrete, and expanded clays and shales in structural concrete. In general, lightweight aggregates are broadly classified into two types of natural and artificial aggregates. Expanded Poly-Styrene (EPS) that is a major waste material in the packaging industry, is frequently used as lightweight aggregate in the LWC preparation (Elzien e*t al.* 2011, AL-Eliwi *et al.* 2017, Herki 2017).

Compressive strength, elastic modulus, splitting tensile strength and other mechanical properties of the LWC are significantly affected by the material properties of the utilized lightweight aggregate. Despite some mixing issues in adding the EPS beads in LWC preparations, they can provide an optimized density and compressive strength to improve the structural efficiency. In the lightweight concrete containing expanded polystyrene beads (EPS-LWC), the smaller size of PES beads in the mixture provides higher compressive strength. However, the higher the EPS volume in the mixture, the lower the durability and mechanical properties of EPS-LWC (Sabaa and Ravindrarajah 1997, Schackow *et al.* 2014).

This type of lightweight concrete can be used as structural and non-structural members in some building applications namely, composite flooring system, cladding panels for curtain walls and load-bearing concrete blocks. It is also used in slabs, where fire protection and structural efficiency (strength to weight ratio) are the main concerns (Haghi *et al*. 2006).

The existing investigations (Park and Chisholm 1999, Babu and Babu 2003, Haghi *et al.* 2006, Miled *et al.* 2007, Bisschop and van Mier 2008, Lepech *et al.* 2008, Bai *et al.* 2011, Chen and Fang 2011, Ling and Teo 2011, Madandoust *et al*. 2011, Sadrmomtazi *et al.* 2012, Xu *et al*. 2012, Trussoni *et al.* 2013, Lo Monte *et al.* 2015, Pecce *et al.* 2015, Ranjbar and Mousavi 2015) and (Bagon and

*Corresponding author, Dr.
E-mail: behnam.vakhshouri@alumni.uts.edu.au

ISSN: 1229-9367 (Print), 1598-6233 (Online)

Frondistou-Yannas 1976, Ravindrarajah and Tuck 1994) give some information about the relationship between the compressive strength and other mechanical properties of structural EPS-LWC. Furthermore, the age factor in development of the mechanical properties of EPS-LWC is not investigated in the literature. The authors have reviewed the considerable amount of existing studies in the literature to investigate the mixture design and mechanical properties of structural and non-structural EPS-LWC during the last 40 years (Vakhshouri and Nejadi 2017). The compressive strength of EPS-LWC was studied in about 85% of the case studies. While, the splitting tensile strength, moduli of rupture and elasticity, shrinkage and stress-strain behavior of EPS-LWC were investigated in about 25% of the case studies. The creep was the least investigated property of EPS-LWC studied in just 2% of the case studies.

This study aims at describing the experimental campaign investigating the mechanical characteristics of the structural EPS-LWC in the fresh and hardened states. The experimental program has been conducted in concrete laboratory of the University of Technology Sydney (UTS).

In terms of the fresh concrete properties, the fresh density and slump value from the mixture design of CC, SCC and LWC are investigated. In the hardened state, the compressive strength, modulus of elasticity, and modulus of rupture, splitting tensile strength, bond –slip behavior from pull-out test, and compressive stress-strain curve are investigated. Moreover, the time-dependent properties of EPS-LWC such as creep and shrinkage strains are evaluated in this study.

The main objectives of this study are as following:

- Description of the mixture design of EPS-LWC and the chemical, physical and mechanical properties of the mixture components;
- Analysis of the experimental results of the tests on fresh and hardened properties of EPS-LWC;
- Proposing the empirical relationships to predict the mechanical properties of LWC;

Verification of the developed relationships with the experimental data.

2. Significance of the research

In the absence of precise experimental results, mechanical properties of LWC with different types of aggregates are generally estimated by the existing models and empirical relationships of CC by modified density effect. In addition, just some properties of LWC are included in the few existing references. Validity of the existing models and empirical relationships of CC and LWC to estimate the mechanical properties of EPS-LWC should be verified. The experimental results and analysis in this study aim at more effectively understanding of the mechanical properties of EPS-LWC, both experimentally and numerically. A wide range of the mechanical properties of EPS-LWC including compressive strength, splitting tensile strength, modulus of rupture, modulus of elasticity, absorbed energy under compression and unconfined compressive stress-strain curve are measured at ages 3, 7, 14, 21, 28, 56 and 91 days and evaluated. The shrinkage data and creep coefficient of EPS-LWC are also investigated for a long period.

3. Experimental program

3.1 Test types and specimens

A wide range of the mechanical properties of EPS-LWC at the hardened state are covered in this study. The experimental program utilized different shapes and sizes of the testing specimen to record the concrete characteristics at different ages. Table 1 shows the performed testing types, shape and size of the testing specimens and the measurements ages for each test type.

Table 2 explains the applied Australian standards and some international codes of practice to determine the mechanical properties of EPS-LWC in the laboratory conditions.

3.2 Materials

3.2.1 Natural aggregates

The mixture design of EPS-LWC in this study contains natural aggregates, artificial lightweight aggregate, cement, water and admixture. Two types of fine and coarse natural aggregates are utilized in the mixture design of EPS-LWC. In the case of fine aggregates, a blend of two types of natural fine aggregates has been used.

3.2.2 Coarse aggregate

The crushed Latite aggregate with a maximum size of 10 mm from Dunmore quarry (NSW, Australia) is used as the natural coarse aggregate. The properties of Dunmore coarse aggregate, including the chemical components and physical and mechanical properties are presented in Table 3. The Australian standards (AS1411 2011) and the Regional Transportation Authority recommendations (RTA-06 2006) were applied in sampling and testing of the aggregates. The applied standards and the allowable range in each case are also shown in Table 2. The properties of Dunmore coarse aggregate are in the allowable range.

3.2.3 Fine aggregates

In this type of LWC, a blend of 50% coarse sand and 50% fine sand provides optimum mix in terms of the density and compressive strength. An equal weight proportion of Peppertree sand with a maximum size of 5 mm, and washed Kurnell Natural River sand with a maximum size of 2 mm was used as fine aggregates in the mixture. The Australian standard (AS1411 2011) and the Regional Transportation Authority (RTA) codes (RTA06 2006) were applied in sampling and testing of the aggregates. The properties of Peppertree-P coarse sand and washed Kurnell Natural River sand are presented in Tables 3 and 4, respectively. Testing and sampling standards are also illustrated in Tables 3 and 4.

Table 1 Shape and size of the EPS-LWC test specimens and test ages

Property	Cylinder (mm)	Cube (mm)	Prism (mm)	Test ages (days)
Compressive strength	150×300	100, 150		3,7, 14, 21, 28, 56, 91
Modulus of elasticity	150×300			3,7, 14, 21, 28, 56, 91
Modulus of rupture			100×100×400	3,7, 14, 21, 28, 56, 91
Splitting tensile strength	100×200,150×300			3,7, 14, 21, 28, 56, 91
Steel-concrete bond	150×300			3,7, 14, 21, 28, 56, 91
Pull-out test	150×300			7, 14, 21, 28, 56, 91
Stress-strain curve				3,7, 14, 21, 28, 56, 91
Creep	150×300			Up to 225 days
Shrinkage			75×75×280	Up to 450 days

Table 2 Applied codes of practice on the curing, sampling and testing the LWC specimens

Property	Test method	Property	Test method
Compressive strength	AS 1012.8.1 (2014) , ASTAM C39 (2000)	Modulus of rupture	AS 1012.8.2 (2014), ASTM C1018 (2002)
Splitting tensile strength	AS 1012.8.1(2014), ASTM C496 (2000)	Steel-concrete bond	RILEM –RC6 (2004)
Creep	AS 1012.16 (2014)	Pull-out test	RILEM –RC6 (2004)
Shrinkage	AS-1012.13 (2014)	Modulus of elasticity	AS 1012.17 (2014), ASTM C469 (2002)

Table 3 Properties of Dunmore 10 mm coarse aggregate

Test method	Test	Allowable	Measured
(AS-1141.11.1 2009)	Passing A.S. sieve (%)		
	13.2 mm	100	100
	9.5 mm	85-100	88
	6.7 mm	40-60	53
	4.75 mm	0-20	20
	2.36 mm	0-5	4
	1.18 mm		2
(AS-1141.12 2011)	≤ 75 µm (%)		1
(AS-1141.14 2011)	Mis-shaped particles (%)		
	Ratio 2:1	<25	23
	Ratio 3:1	<10	6
RMS-T235	Average least dimension (mm)		3.5
	Fraction (-9.5+6.7mm)		6.1
	Fraction (-6.7+4.75mm)		4.4
(AS-1141 2011)	Crushed particles derived from gravel		
	% of crushed particles	≥80	100
	% of uncrushed particles		Nil
(AS-1141.4 2011)	Uncompacted bulk density (t/m3)		1.33
	Compacted bulk density (t/m3)	≥1.2	1.5
RMS-T262	Moisture content (%)		3.0
(AS-1141.6.1 2011)	Particle density (dry) (t/m3)	≥2.1	2.63
	Particle density (SSD) (t/m3)		2.66
	Apparent Particle density (t/m3)		2.76
	Water absorption	<2.5	1.9
(AS-1141.23 2009)	Los Angeles value grading “K” (% loss)	< 30	15
(AS-1141.32 2008)	Weak particles (%)		
	% of original sample passing 2.36 mm (sieve 3.4)	< 0.5	Nil
(AS-1141.25.2 2013)	Degradation factor- coarse aggregate		66
	The washed water after using permitted 500 ml		Not clear

SSD: Saturated Surface-Dry

Table 4 Properties of Peppertree-P coarse sand

Test method	Test	Allowable	Measured
(AS-1141.11.1 2009)	Passing A.S. sieve (%)		
	6.7 mm	100	100
	4.75 mm	95-100	100
	2.36 mm	73-88	80
	1.18 mm	55-70	55
	600 μm	35-50	37
	425 μm		30
	300 μm	25-35	23
	150 μm	10-20	11
AS-1289.4.3.1.	PH value of soil		8.8
AS-1012.20	Chloride as Cl (%)		0.007
	Sulphate as SO3		0.03
(AS-1141.12 2011)	≤ 75 μm (%)	5-10	5
(AS-1141.13 2007)	≤ 2 μm (%)	1	0.7
(AS-1141.4 2011)	Uncompacted bulk density (t/m3)		1.69
	Compacted bulk density (t/m3)	≥1.2	1.86
RMS-T262	Moisture content (%)		0.3
(AS-1141.6.1 2011)	Particle density (dry) (t/m3)	≥2.1	2.69
	Particle density (SSD) (t/m3)		2.71
	Apparent Particle density (t/m3)		2.76
	Water absorption	<2.0	0.9
(AS-1141.32 2008)	Weak particles (%)		
	The % of original sample passing 2.36 mm (sieve 3.4)	< 0.5	0.9
(AS-1141.25.2 2013)	Degradation factor- fine aggregate	≥ 60	85
	The washed water after using permitted 500 ml		clear
AS-1289.3.7.1	Sand equivalent of the soil using a power-operated shaker	≥ 60	76
RMS-T659	Average Methylene blue adsorption value (mg/g)	5	3

Table 5 Properties of washed Kurnell fine sand

Test method	Test	Allowable	Measured
(AS-1141.11.1 2009)	Passing A.S. sieve (%)		
	6.7 mm	100	100
	4.75 mm	90-100	100
	2.36 mm	60-100	100
	1.18 mm	30-100	100
	600 μm	15-100	99
	425 μm		91
	300 μm	5-50	58
	150 μm	0-20	2
AS-1289.4.3.1.	PH value of soil		8.8
AS-1012.20	Chloride as Cl (%)		0.003
	Sulphate as SO3		0.09
AS-1141.12	≤ 75 μm (%)	0-5	Nil
AS-1141.13	≤ 2 μm (%)		Not applicable
AS-1141.31	Light particles (%)		Nil
AS-1141.4	Uncompacted bulk density (t/m3)		1.33
	Compacted bulk density (t/m3)	≥1.2	1.47
RMS-T262	Moisture content (%)		
(AS-1141.6.1 2011)	Particle density (dry) (t/m3)	≥2.1	2.52
	Particle density (SSD) (t/m3)		2.55
	Apparent Particle density (t/m3)		2.59
	Water absorption		1.0
(AS-1141-24 2013)	Sodium Sulphate soundness	< 5.0	
	Total weighted (% loss)	C, B2<12	0.9
	Fraction tested (-600 μm +300 μm (% loss)	A1, A2,B1<15	0.9
AS-1141.33	Silt content (%)		3

SSD: Saturated surface-dry

Table 6 Properties of the Shrinkage Limited (SL) type cement

Test method		Allowable	Measured
	Chemical components		
(AS-2350.2 2006)	LOI (%)	4.3	4.1
	SO3 (%) (AS-2350.2)	< 3.5	3.1
	CI (%) (AS-2350.2)	< 0.10	0.02
	CaO (%)	64.3	62.6
	SiO2 (%)	19.4	19.26
	Al2O3 (%)	5.15	5.15
	Fe2O3 (%)	3.18	3.08
	MgO (%)	1.59	1.14
	K2O (%)	0.51	0.53
	Na2O (%)	0.18	0.08
	P2O5 (%)	0.1	0.05
	Mn2O3 (%)	0.08	0.06
	Physical properties		
(AS-2350.8 2006)	Fineness index (m^2 /kg)	441	395
(AS-2350.3 2006)	Normal consistency (%)		27.7
	Mechanical properties		
(AS-2350.13 2006)	Residue (45 μm)	2.4	
	Drying shrinkage - 28 days mean (με)	< 750	570
(AS-2350.11 2006)	Compressive strength		
	f_c' - 3 days (MPa)		34
	f_c' - 7 days (MPa)	35	45.6
	f_c' - 28 days (MPa)	45	61.1
(AS-2350.4 2006)	Setting time		
	Initial (minute)	≥ 45	105
	Final (minute)	< 600	150
(AS-2350-5 2006)	Soundness	<5 mm	1mm

Table 7 Mix design of lightweight concrete containing expanded polystyrene beads

Component		Proportion
Cement (kg/m^3)		500
Water (liter/ m^3)		180
Water to cement ratio (w/c)		0.36
BST aggregate (Liter/ m^3)		300
Fine aggregate	Coarse sand (kg/ m^3)	310
	Fine sand (kg/ m^3)	310
Coarse aggregate (kg/ m^3)		800
Admixture (liter/ m^3)		2
Mixture volume (m^3)		1.3
Slump (mm)		130
Fresh density (kg/m^3)		2000

Table 8 Test methods to determine the fresh properties of LWC

	Curing	Sampling	Slump test	Mass per volume
Test method	AS-1012.8 (2014)	AS-1012.1 (2014)	AS1012.3.1 (2014)	AS1012.5 (2014)

Table 9 Mechanical properties of EPS lightweight concrete mixture at different ages

Age (day)	3	7	14	21	28	56	91
Compressive strength (MPa)	14.49	25.38	27.93	29.62	30.96	32.33	33.3
Splitting tensile strength (MPa)	1.44	2.3	2.6	2.78	2.89	2.98	3.08
Modulus of elasticity (GPa)	11.63	15.68	17.65	19.48	20.32	21.1	21.89
Ultimate rupture load (KN)	9.94	11.66	13.52	14.06	14.35	14.58	15.08
Modulus of rupture (MPa)	2.982	3.498	4.056	4.218	4.305	4.374	4.524

Fig. 1 BST aggregates (expanded polystyrene beads) in fresh lightweight concrete

3.2.4 Artificial lightweight aggregate

The low-density foam of expanded polystyrene is used as lightweight aggregate to reduce the density of concrete. EPS is a closed-cell lightweight cellular plastic material produced from polystyrene. The material has been modified by addition of the flame-retardant additives. The expandable foam is produced in the form of small beads. “BST” aggregate is a commercial name for the used spherical-shaped polystyrene beads with hydrophobic type chemical coating. The percentage passing of the BST beads on 4.75 mm and 2.36 mm sieves were 100% and 90%, respectively. Bulk and particle density of the beads were 35 and 67 kg/m3, respectively. Fig. 1 shows the BST aggregates and the fresh LWC concrete mixture containing the BST beads utilized in this study.

3.2.5 Admixtures

According to the Australian standard (AS-1478.1 2000) provisions, the lignosulfonates based Plastiment20 is used as high range water reducing agent. This admixture helps to achieve increased workability without loss of strength and also to increase the strength without loss of workability. The time period during which the concrete can be placed is also extended. There are no other super plasticizer and viscosity modifying agent used in the mixture.

3.2.6 Cement

BST concrete mix design is based on the Shrinkage Limited (SL) cement confirming (AS-3972 2010) and (AS-2350 2006) provisions. This cement is a special and modified type of the General Purpose (GP) cement and contains up to 7.5% additional limestone mineral powder. Other types of cement are suitable, but their effect on yield and performance of the mixture should be determined. The chemical, physical and mechanical properties of the used SL (GP) type cement are presented in Table 6.

Despite advantages of EPS-LWC in the construction industry, the huge amount of Portland cement in its mixture design is a negative point to increase the environmental and energy consumption concerns. However, the amount of cement is required to decrease the water to cement ratio for higher strength demand in the structural type of EPS-LWC.

3.2.7 Mixture proportions

The consistent materials and corresponding mixture proportions to achieve a structural EPS-LWC with low density is presented in Table (7). This slump value provided the required flow-ability and workability to pour the fresh concrete in the test specimens. Additionally, to avoid any blocking problem, the maximum size of the coarse aggregate was restricted to 10 mm in the mixture.

Table 8 shows the Australian standard (AS-1012 2014) applied to curing, sampling, slump test and mass per volume measurements of the fresh EPS-LWC in this study.

3.3 Preparation and curing condition of test specimens

All specimens were cast within 15 minutes after the end of the mixing process. The fresh concrete was poured into the molds in 2 or 3 layers following the seconds of vibration by the vibrating table. Vibrating the concrete over 5 seconds causes the EPS beads to float up to the concrete surface. After casting, specimens were carefully moved and kept covered in a controlled chamber at 23±2°C conforming (AS-1210.8.1 2014), up to the demolding time after 24 hours. Then, all test specimens were stored in the water pre-saturated with lime until the measurement time Table 1.

4. Experimental results

4.1 Compressive strength

Fig. 2 show the testing set-up and the EPS-LWC specimens used to determine the compressive strength, splitting tensile strength, modulus of elasticity, modulus of rupture, shrinkage strain and direct tension strength in the laboratory conditions. Preparation and comparative size and shape of the test specimens, failure mode and measurement devices are also shown in Fig. 2. Table 9 presents the recorded experimental values of the compressive strength, splitting tensile strength, moduli of elasticity and rupture and ultimate rupture load (flexural test) in EPS-LWC at different ages. The loading rate and measurement points agree with the standards pertaining to each test.

The results show that the compressive strength at ages 3 and 7 days is 46.79% and 82.97% of the compressive strength at age 28 days, respectively. The compressive strength at ages 56 and 91 days is 4.4% and 7.64% higher than that of 28 days, respectively. In other words, the main development of the compressive strength up to 45% occurs at early age (up to 3 days).

4.2 Splitting tensile strength

Experimental values of the splitting tensile strength of EPS-LWC at different ages are presented in Table 9. The splitting tensile strength at ages 3, 7, and 14 days is 49.9%, 79.5% and 89.9% of the splitting tensile strength at age 28 days, respectively. Moreover, the splitting tensile strength at ages 56 and 91 days is about 3% and 6% higher than that of 28 days, respectively. According to the test results, EPS-LWC gains about 50% of the final splitting tensile strength at age 3 days. In addition, there is no considerable development of the splitting tensile strength of EPS-LWC after 28 days.

4.3 Modulus of elasticity

Experimental values of the modulus of elasticity of

Fig. 2 Testing setup and specimens for (a) compressive strength, (b) splitting tensile strength,(c) modulus of rupture, (d) modulus of elasticity, (e) pull-out and (f) shrinkage at different ages

EPS-LWC at different ages are presented in Table 9. The modulus of elasticity at ages 3, 7, and 14 days is 57.2%, 77.2% and 86.9% of the modulus of elasticity at age 28 days, respectively. Furthermore, the experimental values of the modulus of elasticity at ages 56 and 91 days are about 1.03% and 1.08% higher than that of 28 days, respectively.

According to the test results, the main part of the development of modulus of elasticity of EPS-LWC happens at age 3 days. There is no meaningful improvement of the modulus of elasticity of EPS-LWC after age 28 days.

4.4 Modulus of rupture (Flexural strength)

The main objectives of this test are to determine the flexural toughness and cracking strength of EPS-LWC. Table 9 shows the experimental values of the modulus of rupture and ultimate rupture load at different ages. The modulus of rupture at ages 3, 7 and 91 days is 69%, 81% and 105% of that at age 28 days, respectively. In other words, EPS-LWC gains the main part of its modulus of rupture at the early ages.

The mid-span deflection of the flexural test specimens under the third-point loading is also recorded by a transducer installed under the prism specimen. Fig. 3 compares the load-deflection curves at mid-span of the test prisms at ages 7, 28 and 56 days.

Despite similar ascending trend of the load-deflection diagram at all ages, for the same loading rate and extent, the flexural deflection at fracture point is considerably low at early-age of the plain concrete. The rupture load at 56 days is about 2% higher than that of 28 days; however, the corresponding mid-span deflection at 28 days is about 25% higher. This difference can be explained as result of the higher flexural stiffness of the concrete specimen at 56 days. The rupture load and maximum deflection at age 7 days are considerably below those of 28 days.

4.5 Pull-out test

Table 10 shows the testing specimen details, cracking status and the experimental bond-slip between the concrete and steel bars in the pull-out test. Depending on the steel bar-concrete bond quality, different failure modes may happen in this test. In lower level of the bar-concrete bond, the pull-out (slipping) failure mode is the most probable. While, in higher bond levels the cone failure, edge failure and splitting failure may happen due to the tensile loading.

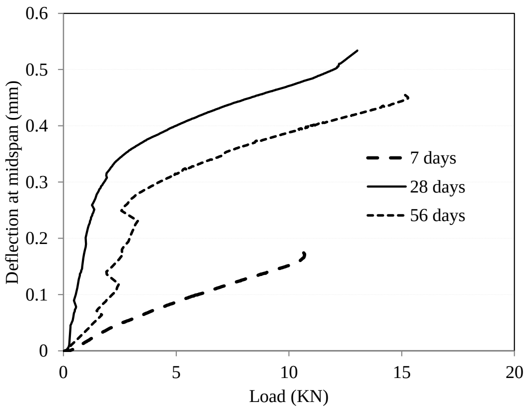

Fig. 3 Load-deflection in mid-span of the flexural test specimens at different ages

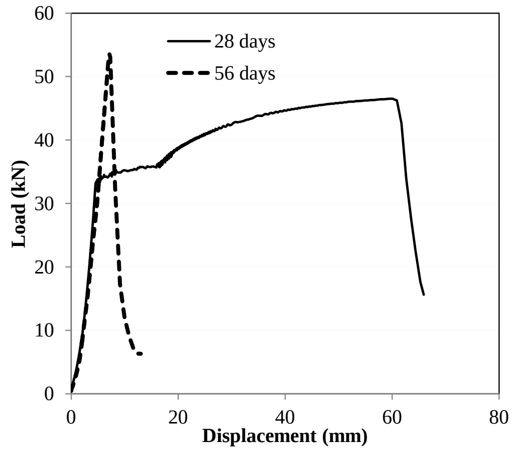

Fig. 4 Brittle and ductile failure of pull-out test specimens at 28 and 56 days

In Table 10, l_d and d_b are the embedded length and diameter of the tension bar in middle of the cylindrical specimen. F_u is the ultimate tension load to failure the specimen. The ultimate load caused cracking of the surrounded concrete with slip of the steel bar in the mature concrete at ages 28, 56 and 91 days. While, in the young concrete at ages 3, 7, 14 and 21 days, the slip of steel bars under the ultimate tension load caused no crack in the surrounded concrete. The improved bond between the concrete and steel bar in the specimens at ages 28, 56 and 91 days is the main reason to cracking of the cylinders.

The steel-concrete bond stress ate ages 3, 7 and 14 days is 70.4%, 84.3 and 91.7% of that at age 28 days, respectively. The bond stress at ages 56 and 91 days is about 8% and 12% higher than that of 28 days, respectively.

Fig. 4 compares the load-displacement curves of the pull-out test specimens at ages 28 and 56 days. The failure mode of specimen at age 56 days is brittle, while the specimen at age 28 days shows a ductile failure. In the 28 days specimen, the steel bar is pulled out with minor cracking in the concrete cylinder; while, in the specimen tested at 56 days, slip of the steel bar occurs with considerable splitting cracking of the cylinder around the embedded bar.

Eq. (1) is proposed to describe the relationship between the bond stress and slip in a reinforced EPS-LWC member under direct tension.

$$\tau = 62.928\ s^{-0.399} \tag{1}$$

Where; "τ" is bond stress (MPa) and "s" is the slip of steel bar under tension (mm).

4.6 Unconfined compressive stress-strain curve

To obtain the complete Compressive Stress-Strain Curve (CSSC) of EPS-LWC, the cylindrical specimens were subjected to compression tests with a carefully controlled displacement rate. The compressive stress-strain curves at ages 14 and 28 days are presented in Fig. 5. The general trend of CSSC is similar at ages 14 and 28 days. However, due to the lower elasticity of hardened concrete at 14 days,

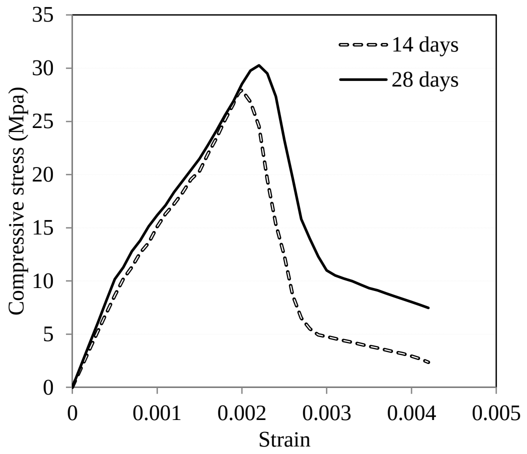

Fig. 5 Stress-strain diagram of the LWC mixture at different ages

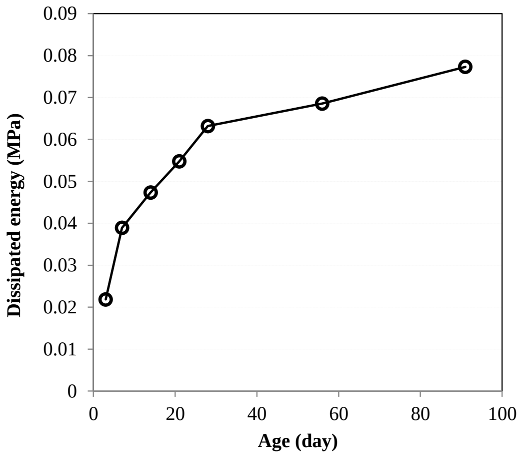

Fig. 6 The energy stored in unit volume of EPS-LWC under compression at different ages

the specimen shows higher strain values under the compressive stress. The ascending part of CSSC at both ages is comparable; however, there are some differences on the descending part. The peak stress point at age 14 days is lower than that of 28 days; however, the ultimate strain at both ages is 0.0042.

The higher content of cement in the mixture and lower stiffness of the EPS beads result in larger deformation of EPS-LWC specimen. In comparison with the ordinary concrete, these characteristics in EPS-LWC cause more ductile stress-strain changes.

4.7 Energy absorption under compression

The applied work on concrete is stored as elastic and plastic energy. The elastic energy is recovered deformation energy; while, the plastic energy is consumed to initiate and develop cracks during failure.

The absorbed energy is equal to the area under the compressive stress-strain curve up to the failure point. Eq. (2) is utilized to calculate the absorbed energy per unit volume of the cylindrical EPS-LWC specimens under compression at different ages.

$$\mathrm{G_c} = \int_0^{\varepsilon_u} \sigma . d\varepsilon \tag{2}$$

Where; G_c is absorbed energy per unit volume (MPa), σ is compressive stress (Mpa), ε is strain, and ε_u is the ultimate strain.

According to Fig. 5, the ultimate strain in calculation of the stored energy at different ages is taken as 0.0042. Fig. 6 also compares the absorbed energy in compressive cylinders at different ages. Evidently, G_c is increasing in the EPS-LWC by increasing the age of concrete. The G_c values at ages 3, 7 and 91 days are 34.6%, 61.5% and 122% of the G_c at 28 days, respectively. As shown in Fig. 6, there is no significant change in the stored energy after 28 days. Considering the effect of low elasticity of EPS-LWC on the strain changes, development rate of G_c is different from development rate of the compressive strength.

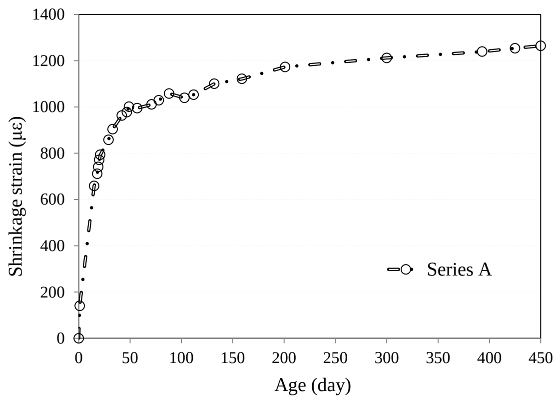

Fig. 7 Development of the shrinkage strain of EPS-LWC with time

4.8 Drying shrinkage

Fig. 7 shows the development of shrinkage strain of EPS-LWC with time. The specimens were moist-cured for a week before measurement of the shrinkage strain. The experimental shrinkage strain after 450 days is in the range of 1200-1300 με. While, the main part of the shrinkage strain development (about 70%) happens before the age 50 days.

4.9 Creep coefficient of lightweight concrete

The creep coefficient of EPS-LWC was measured for 225 days under two distinct levels of uniform compressive stress equal to $0.3f_c'$ and $0.4f_c'$. Each creep rig containing two cylindrical specimens was subjected to loading at age 14 days. Fig. 8 shows the specimen and testing equipment used to measure the creep coefficient of EPS-LWC.

Fig.e 9 shows the creep coefficients under two levels of sustained loads at different ages for EPS-LWC specimens. The final creep coefficient after 225 days under load levels $0.3f_c'$ and $0.4f_c'$ was 2.231 and 2.415, respectively. The maximum creep coefficient of specimens subjected to higher load level is 8.2% higher than that of lower load level.

Fig. 9 shows the creep coefficients under two levels of sustained loads at different ages for EPS-LWC specimens. The final creep coefficient after 225 days under load levels $0.3f_c^{\prime}$ and $0.4f_c^{\prime}$ was 2.231 and 2.415, respectively. The maximum creep coefficient of specimens subjected to higher load level is 8.2% higher than that of lower load level.


(a)


(b)

Fig. 8 Creep test rig at two different load levels

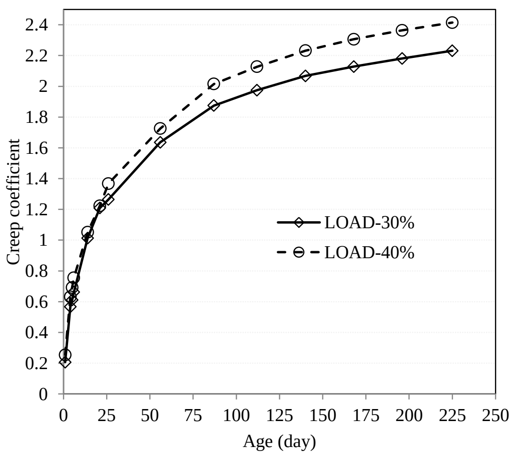

Fig. 9 Creep coefficients of EPS-LWC under two different load levels

Table 10 Specimen dimensions and variables of pull-out test

Age (day)	F_u (KN)	Slip, s (mm)	l_d (mm)	d_b (mm)	Bond stress, τ(MPa)	Presence of cracking
3	33.52	33.3	150	12	14.83	Un-cracked
7	40.17	25.3	150	12	17.77	Un-cracked
14	43.69	21.3	150	12	19.33	Un-cracked
21	45.57	17.7	150	12	20.16	Un-cracked
28	47.6	15	150	12	21.08	Cracked
56	51.7	11.3	150	12	22.87	Cracked
91	53.64	12.3	150	12	23.73	Cracked

5. Proposed analytical relationships

5.1 Time-related mechanical properties

Mechanical properties of concrete are developing with time by different rates. However, this rate is different for corresponding characteristics in different types of concrete. The mathematical models are effective tools to express the developments of mechanical properties of concrete with time. Utilizing regression analysis of the experimental data, the empirical relationships in Eqs. (3) to (7) are proposed to predict the compressive strength, splitting tensile strength, modulus of elasticity, modulus of rupture and absorbed energy per unit volume of EPS-LWC at different ages, respectively. Efficiency of the predictions of the proposed models, compared to the experimental time-related data is evaluated in Fig. 10. The diagrams in Fig. 7 confirm the good agreement between the experimental results and estimated values of the compressive strength, modulus of elasticity, modulus of rupture and splitting tensile strength of EPS-LWC by the proposed empirical equations.

5.1.1 Compressive strength

$$f_c^{\prime}(t) = (0.1633 \ln t + 0.417)\, f_{c-28}^{\prime} \tag{3}$$

Where; $f_c^{\prime}(t)$ is the compressive strength (MPa) at age t (days) and $f_{c-28}^{\prime}$ is the compressive strength (MPa) at age 28 days.

According to Fig. 10, Eq. (3) underestimates the values for compressive strength under the age of 28 days, while it overestimates the compressive strength for 56 and 91 days, to some extent. However, the difference between the predicted and experimental values is not significant.

5.1.2 Splitting tensile strength

$$f_{ct}(t) = (0.156 \ln t + 0.4341)\, f_{ct-28} \tag{4}$$

Where; $f_{ct}(t)$ is the splitting tensile strength (*MPa*) at age t (days), and f_{ct-28} is the splitting tensile strength (*MPa*) at age 28 days.

As presented in Fig. 10, the predicted values of splitting tensile strength by the Eq. (4) are in good agreement with the experimental data.

5.1.3 Modulus of elasticity

$$E_c(t) = (0.1467 \ln t + 0.4666)\, E_{c-28} \quad (5)$$

Where; $E_c(t)$ is the modulus of elasticity (*GPa*) at age *t* (days) and E_{c-28} is the modulus of elasticity (*GPa*) at age 28-days.

The predicted values by Eq. (5) are in agreement with the experimental values of modulus of elasticity in Fig. 10.

5.1.4 Modulus of rupture

$$f_r(t) = (0.1046 \ln t + 0.62)\, f_{r-28} \quad (6)$$

Where; $f_r(t)$ is the modulus of rupture (*MPa*) at age *t* (days) and f_{r-28} is the modulus of rupture (*MPa*) at age 28-days.

The predicted values of the modulus of rupture by Eq. (6) are in good agreement with the experimental data in Fig. 10.

5.1.5 Absorbed energy under compression

The absorbed energy per unit volume of the EPS-LWC specimen under compression at different ages can be expressed by Eq. (7).

$$G_c(t) = (0.016 \ln t + 0.0061)\, G_{c-28} \quad (7)$$

Where; $G_c(t)$ is the stored energy per unit volume of the specimen (*MPa*) at age t (days) and G_{c-28} is stored energy per unit volume of the specimen (*MPa*) at age 28 days.

According to Fig. 11, the Eq. (7) gives reasonable predictions of the absorbed energy per unit volume of EPS-LWC specimen under compression.

Variation of the stored energy per unit volume of EPS-LWC under compression with the strain changes at different ages is shown in Fig. 12. The G_c-ε diagrams in Fig. 12 for different ages indicate the higher rate of G_c increment with strain by increasing the age of the specimen. In other words, the older specimens demonstrate a more rapidly development of the stored energy per unit volume of the EPS-LWC specimen.

5.1.6 Creep strain

The creep of EPS-LWC is investigated under two distinct levels of compressive stress. The sustained compressive stress at two load levels is $0.3f'_c$ and $0.4f'_c$, respectively. Eq. (8) describes the creep strain of EPS-LWC at different ages under two different levels of sustained stress.

$$\varepsilon_{cr} = 800\alpha t^{\beta} \quad (8)$$

Where; ε_{cr} is creep strain, α is the ratio of applied stress to the compressive strength of concrete, β is the coefficient of time.

The age of specimen and magnitude of the sustained stress (fraction of the compressive strength of concrete) are included in Eq. (8). Considering the number of concrete mixtures used in this study, inclusion of the other effective parameters of creep strain in Eq. (8) will not be practical.

Table 11 Coefficients of creep strain Eq. (9)

Sustained stress (MPa)	a	b	c	α	β
$0.3f'_c$	0.65	8	0.6	0.3	0.375
$0.4f'_c$	0.75	10	0.72	0.4	0.375

Eq. (9) is proposed in this study to predict the creep coefficient of EPS-LWC subjected to different levels of sustaining compressive stress. The coefficients of each load level in Eqs. (8) and (9) are shown in Table 11.

$$\phi(t, t_0) = \frac{t^a}{b + t^c}\phi_u \quad (9)$$

Where; $\phi(t, t_0)$ is creep coefficient, ϕ_u is ultimate creep coefficient, and *a, b, c* are experimental parameters.

Figs. 13(a) and 13(b) confirm the efficiency of the proposed equations in this study to predict the creep strain of EPS-LWC under different levels of sustained stress.

Fig. 14 confirms efficiency of the proposed equations in this study to predict the creep coefficient of EPS-LWC under different levels of sustaining compressive stress.

5.1.7 Shrinkage strain

Development of shrinkage strain of EPS-LWC in this study is the most compatible with the predictions of the proposed empirical relationship in Eq. (10). It is based on the model proposed by (Best and Polivka 1959) to estimate the shrinkage strain in lightweight concrete

$$\varepsilon_{sh} = 188 \times t^{0.315} \quad (10)$$

Where; ε_{sh} is the shrinkage strain ($\mu\varepsilon$) and *t* is the age of shrinkage specimen (*days*) after one-week moist curing.

Efficiency of the proposed relationship in Eq. (10), compared to the experimental data and estimated shrinkage strain by some main models of lightweight concrete is presented in Fig. 15.

5.2 Compressive strength-related analytical models

Compressive strength is the fundamental parameter of the hardened concrete to determine its other mechanical properties. Tables 9 and 10 summarize the experimental data for the mechanical properties of EPS-LWC at different ages. Based on the regression analysis of the experimental data, Eqs. (11) to (14) are proposed to estimate the splitting tensile strength, modulus of elasticity, modulus of rupture and ultimate pull-out load of EPS-LWC from the compressive strength. According to Figs. (16), the proposed equations to predict the splitting tensile strength, modulus of elasticity and modulus of rupture are in good agreement with the experimental data. The correlation factor (R^2) in each equation confirms the accuracy of the proposed equations, compared to the experimental data.

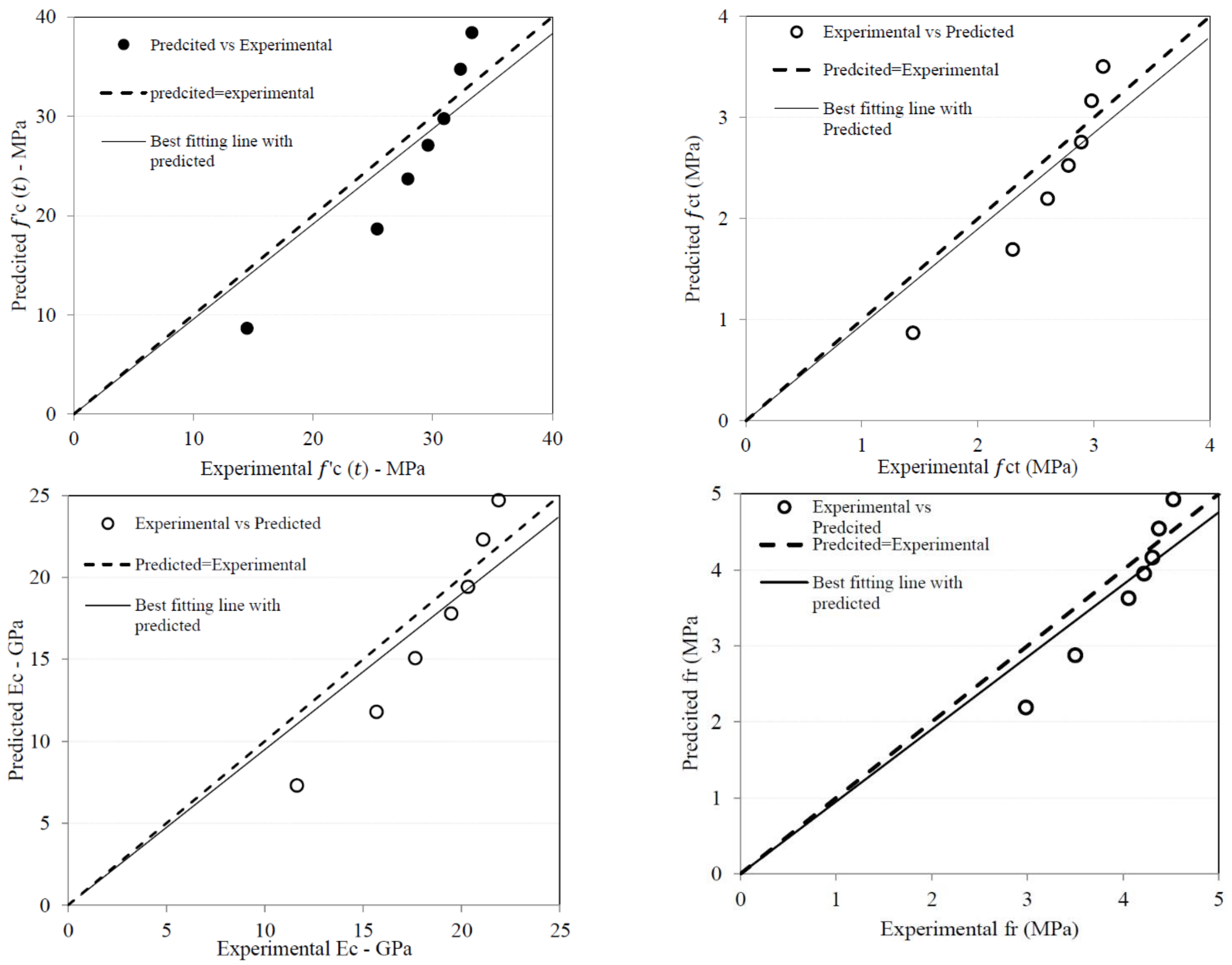

Fig. 10 Experimental vs. predicted values of compressive strength, splitting tensile strength, modulus of elasticity and modulus of rupture

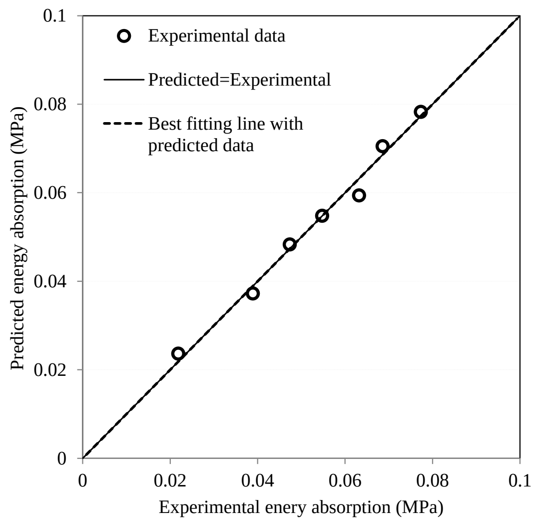

Fig. 11 Predicted versus experimental energy absorption under compression

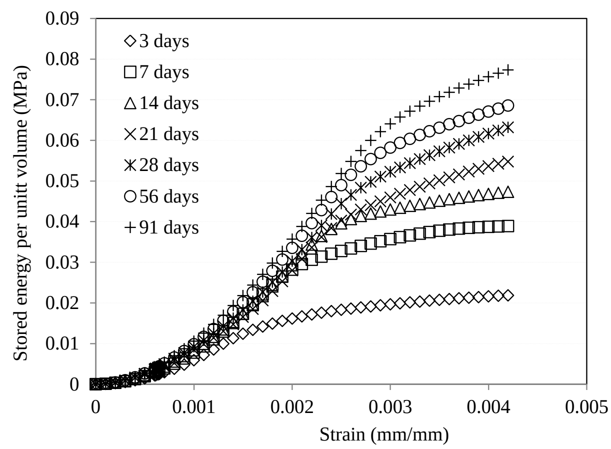

Fig. 12 Stored energy under compression versus strain of EPS-LWC at different ages

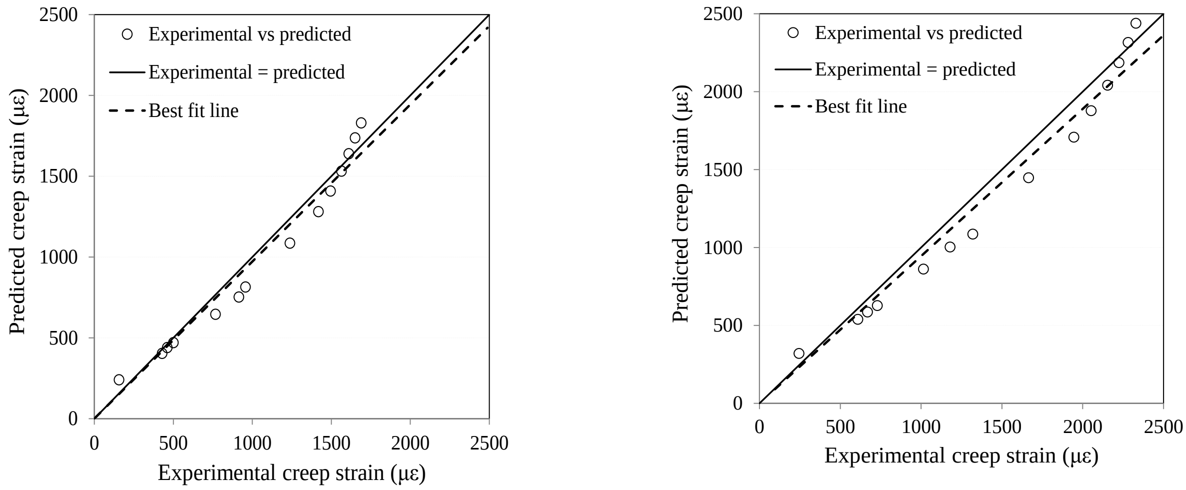

(a) (b)

Fig. 13 Experimental vs. predicted creep strain under sustained stress of (a) $0.3f_c'$ and (b) $0.4f_c'$

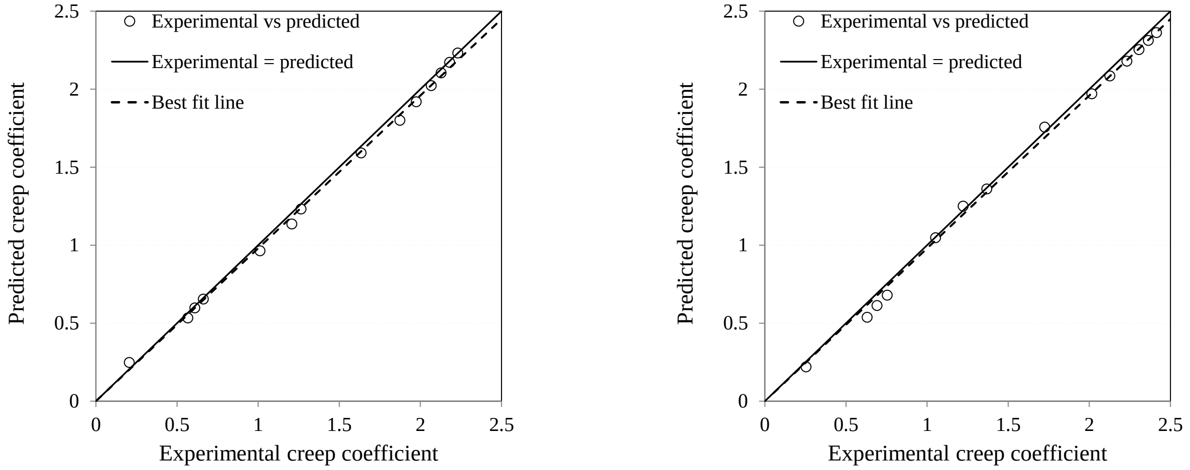

(a) (b)

Fig. 14 Experimental vs. predicted creep coefficient under sustained stress of (a) $0.3f_c'$ and (b) $0.4f_c'$

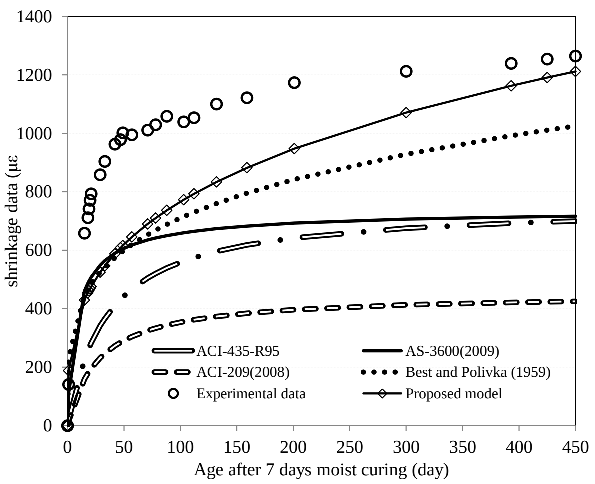

Fig. 15 Experimental data of EPS-LWC vs. predicted shrinkage strain by different models

5.2.1 Splitting tensile strength

Eq. (11) is proposed to predict the splitting tensile strength of EPS-LWC at different ages

$$f_{tc} = 0.1227 \times {f_c'}^{0.9176} \quad R^2 = 0.996 \tag{11}$$

5.2.2 Modulus of elasticity

Eq. (12) is proposed to predict the modulus of elasticity of EPS-LWC at different ages

$$E_c = 1.5045 \times {f_c'}^{0.7523} \qquad R^2 = 0.987 \tag{12}$$

5.2.3 Modulus of rupture

Eq. (13) is proposed to predict the modulus of rupture (flexural tensile strength) of EPS-LWC at different ages.

$$f_r = 0.7625 \times {f_c'}^{0.5003} \tag{14}$$

5.2.4 Ultimate pull-out load

Eq. (14) is developed to explain the relationship between the ultimate pull-out load and the compressive strength of EPS-LWC.

$$F = 0.9925f'_c + 17.481 \qquad R^2 = 0.96 \tag{14}$$

Where; F is the ultimate pull-out load (KN) and f'_c is the compressive strength (MPa).

5.2.5 Compressive stress-strain relationship

The relation between the compressive stress and strain in the EPS-LWC specimens in this study is described by the Eq. (15). In the proposed relationship for compressive stress-strain curve, the Eqs. (3) and (12) proposed for the time-dependent compressive strength and modulus of elasticity are also utilized.

$$\sigma_c = \frac{f'_c.\,\beta(\varepsilon/\,\varepsilon_0)}{[(\beta - 1 + (\varepsilon/\,\varepsilon_0)^{\beta}]} \quad ;\ 0 \le \varepsilon \le\ \varepsilon_{max} \tag{15}$$

$$\beta = \frac{1}{1 - \frac{f'_c}{E_0\varepsilon_0}}$$

$$\sigma_c = \frac{f'_c.\,n\beta(\varepsilon/\,\varepsilon_0)}{[(n\beta - 1 + (\varepsilon/\,\varepsilon_0)^{n\beta}]} \quad \text{if}\ \ \varepsilon > \varepsilon_0$$

$$n = 0.0012P^2 - 0.0846P + 1.551$$

$$P = \frac{Esec}{E_0} \qquad Esec = \frac{f'_c}{\varepsilon_0}$$

$$\varepsilon_0 = 6.52f'_c \times 10^{-5} + 1.634 \times 10^{-4}$$

$$E_0 = 1.5045 \times {f'_c}^{0.7523}$$

Where; σ_c and ε are stress and strain of concrete, f'_c, ε_0 are maximum stress and corresponding strain of concrete, β is material parameter and E_0 is initial tangent modulus of elasticity.

Fig. (17) compares the experimental versus predicted values of the strain in EPS-LWC under different levels of the compressive stress.

6. Verification of the proposed equations

The authors have conducted a comprehensive review on the mechanical properties of EPS-LWC since it was applied in the research investigations and industrial projects in 1976 (Vakhshouri and Nejadi 2017). Based on real experimental data of 154 EPS-LWC mixture designs from 55 experimental investigations, they proposed and verified equations to describe the mechanical properties of structural and non-structural EPS-LWC. Considering the compressive strength and density of the used EPS-LWC in this study, the equations for structural EPS-LWC is utilized to verification of the proposed models in this study. Table 12 shows the compatibility of the proposed relationships in this study with the existing models in the literature. The least square method in regression analysis is used to calculate the compatibility between the predicted values in the proposed model and the best matching model in the reference in Table 12.

Table 12 Compatibility of the proposed relationships with the existing models

Mechanical property	Reference model	Compatibility
Modulus of elasticity	(ACI-209-2R 2008)	81%
Splitting tensile strength	(Bogas and Nogueira 2014)	74%
Modulus of rupture	(Yusuf and Jimoh 2013)	83%
Bond-slip	(Malvar *et al.* 2003)	80%
Maximum bond stress	(Kim *et al.* 2013)	78%
Compressive stress-strain	(Hussin *et al.* 2013)	69%
Shrinkage strain	(Best and Polivka 1959)	89%
Creep coefficient	(Sabaa and Ravindrarajah 1997)	78%

7. Conclusions

The results of an experimental campaign on the engineering properties at different ages of the lightweight concrete containing expanded polystyrene beads are presented and commented, with reference to the compressive strength, modulus of elasticity, modulus of rupture, splitting tensile strength, bond-slip between steel bar and concrete, energy absorption and stress strain response of the structural EPS-LWC in compression. The following conclusions can be drawn:

- New empirical relationships are proposed to predict the variation of the compressive strength, splitting tensile strength, modulus of rupture, modulus of elasticity, bond-slip behavior, absorbed energy and compressive stress-strain of EPS-LWC as a function of time. The proposed relationships are in good agreement with the experimental data;
- Analytical equations are proposed to express the relationship of the compressive strength of EPS-LWC with splitting tensile strength, modulus of elasticity, modulus of rupture, steel-concrete bond stress, ultimate pull-out load, absorbed energy and compressive stress-strain. Predictions of the empirical relationships are in good agreement with the experimental data;
- Strength development of EPS-LWC happens rapidly at early-age, compared to later ages. Based on the experimental results of this study, the main part of the development of the compressive strength, splitting tensile strength, flexural strength and modulus of elasticity of EPS-LWC occurs at early age (about 3 days). There is no considerable development in the mechanical properties of EPS-LWC after 28 days;
- In EPS-LWC the compressive strength at 3 days after casting is 45% of the nominal strength at 28 days, compared to the corresponding range of 35-40% in ordinary concrete;
- The splitting tensile strength of EPS-LWC at 3 days after casting is 50% of that at 28 days;

The modulus of elasticity of EPS-LWC at 3 days after casting is 57% of that at 28 days;

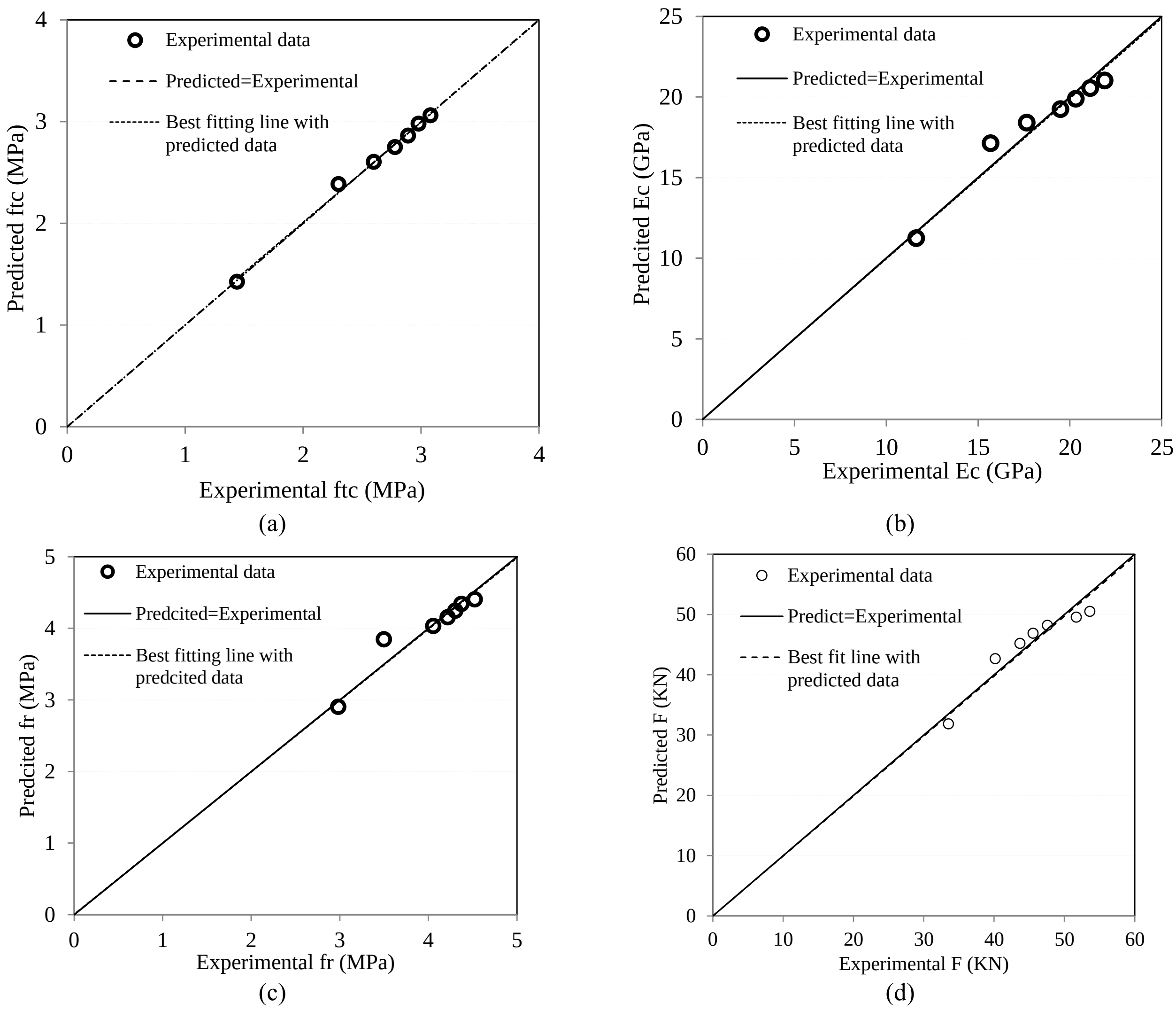

Fig. 16 Predicted versus experimental values of (a) splitting tensile strength, (b) modulus of elasticity, (c) modulus of rupture and (d) Ultimate pull-out load of EPS-LWC

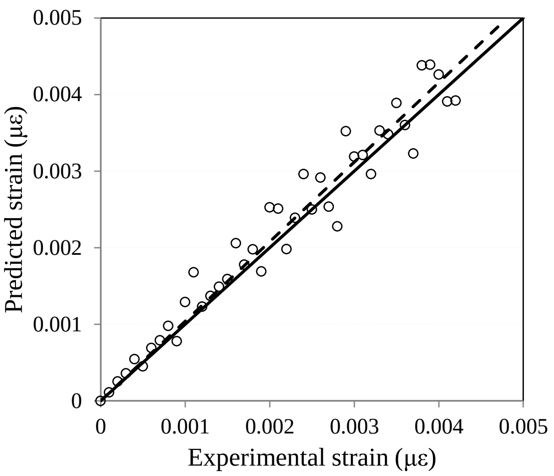

Fig. 17 Comparison of the measured and predicted strain under different values of compressive stress

- In EPS-LWC the modulus of rupture at 3 days after casting is 69% of that at 28 days;
- The steel-concrete bond stress of EPS-LWC at 3 days after casting in EPS-LWC is 70% of that at 28 days, compared to 80% in ordinary concrete;
- The rate of shrinkage strain development and magnitude of the ultimate shrinkage strain in EPS-LWC is about twice those of ordinary concrete;
- The shrinkage strain of EPS-LWC is developing from 900με at age 50 days to its ultimate value of 1200με, compared to about 500με of ultimate shrinkage strain in ordinary concrete;
- The creep coefficient of EPS-LWC under the stress levels equal to $0.3f_c'$ and $0.4f_c'$ is 2.231 and 2.415, respectively.

Lower stiffness of EPS beads and considerable cement content in the mixture cause more ductile behavior under compression.

References

ACI-209-2R (2008), "Guide for Modeling and Calculating Shrinkage and Creep in Hardened Concrete", Reported by ACI Committee 209.

AL-Eliwi, B., Ekmekyapar, T., Faraj, R., Göğüs, M. and AL-Shaar, A. (2017), "Performance of lightweight aggregate and self-compacted concrete-filled steel tube columns", *Steel Compos. Struct.*, **25**(3), 299-314. https://doi.org/10.12989/scs.2017.25.3.299.

AS-1012 (2014), "Methods of testing concrete", Standards Australia, Sydney, Australia.

AS-1141-24 (2013), "Methods for sampling and testing aggregates - Aggregate soundness - Evaluation by exposure to sodium sulphate solution", Standards Australia, Sydney, Australia.

AS-1141 (2011), "Methods for sampling and testing aggregates", Standards Australia, Sydney, Australia.

AS-1141.4 (2011), "Methods for sampling and testing aggregates - Bulk density of aggregate", Standards Australia, Sydney, Australia.

AS-1141.6.1 (2011), "Methods for sampling and testing aggregates - Particle density and water absorption of coarse aggregate - Weighing-in-water method", Standards Australia, Sydney, Australia.

AS-1141.11.1 (2009), "Methods for sampling and testing aggregates - Particle size distribution - Sieving method", Standards Australia, Sydney, Australia.

AS-1141.12 (2011). "Methods for sampling and testing aggregates - Materials finer than 75 um in aggregates (by washing)", Standards Australia, Sydney, Australia.

AS-1141.13 (2007), "Methods for sampling and testing aggregates - Material finer than 2 micrometer", Standards Australia, Sydney, Australia.

AS-1141.14 (2011), "Methods for sampling and testing aggregates - Particle shape, by proportional caliper", Standards Australia, Sydney, Australia.

AS-1141.22 (2008), "Methods for sampling and testing aggregates - Wet/dry strength variation", Standards Australia, Sydney, Australia.

AS-1141.23 (2009), "Methods for sampling and testing aggregates - Los Angeles value", Standards Australia, Sydney, Australia.

AS-1141.25.2 (2013), "Methods for sampling and testing aggregates - Degradation factor - Coarse aggregate", Standards Australia, Sydney, Australia.

AS-1141.32 (2008), "Methods for sampling and testing aggregates - Weak particles (including clay lumps, soft and friable particles) in coarse aggregates", Standards Australia, Sydney, Australia.

AS-1141.34 (2007), "Methods for sampling and testing aggregates - Organic impurities other than sugar", Standards Australia, Sydney, Australia.

AS-1141.35 (2007), "Methods for sampling and testing aggregates - Sugar." Standards Australia, Sydney, Australia.

AS-1210.8.1 (2014), "Methods of testing concrete- Method 8.1: method for making and curing concrete, compression and indirect tensile test specimens", Standards Australia, Sydney, Australia.

AS-1411 (2011), "Methods for sampling and testing aggregates, particle size distribution-sieving method", Standards Australia, Sydney, Australia.

AS-1478.1 (2000), "Methods for sampling and testing aggregates, particle size distribution-sieving method", Standards Australia, Sydney, Australia.

AS-2350-5 (2006), "Methods of testing portland, blended and masonry cements - Determination of soundness", Australian Standard.

AS-2350 (2006), "Methods of testing Portland and blended cements", Standards Australia, Sydney, Australia.

AS-2350.2 (2006), "Methods of testing portland, blended and masonry cements - Chemical composition", Australian Standard.

AS-2350.3 (2006), "Methods of testing portland, blended and masonry cements - Normal consistency", Standards Australia, Sydney, Australia.

AS-2350.4 (2006), "Methods of testing portland, blended and masonry cements - Setting time", Standards Australia, Sydney, Australia.

AS-2350.8 (2006), "Methods of testing portland, blended and masonry cements - Fineness index by air permeability method", Australian standard.

AS-2350.11 (2006), "Methods of testing portland, blended and masonry cements - Compressive strength", Standards Australia, Sydney, Australia.

AS-2350.13 (2006), "Methods of testing portland, blended and masonry cements - Determination of drying shrinkage of cement mortars", Standards Australia, Sydney, Australia.

AS-3972 (2010), "General purpose and blended cements", Standards Australia, Sydney, Australia.

Babu, K.G. and Babu, D.S. (2003), "Behaviour of lightweight expanded polystyrene concrete containing silica fume", *Cement Concrete Res.*, **33**(5), 755-762. https://doi.org/10.1016/S0008-8846(02)01055-4.

Bagon, C. and Frondistou-Yannas, S. (1976), "Marine floating concrete made with polystyrene expanded beads", *Mag. Concrete Res.*, **28**(97), 225-229.

Bai, E.L., Xu, J.Y. and Gao, Z.G. (2011), Study on Deformation Property of EPS Concrete Under Impact Loading, Applied Mechanics and Materials, Trans Tech Publ.

Best, C.H. and Polivka, M. (1959), "Creep of lightweight concrete", *Mag. Concrete Res.*, **11**, 129-134.

Bisschop, J. and van Mier, J.G. (2008), "Effect of aggregates and microcracks on the drying rate of cementitious composites", *Cement Concrete Res.*, **38**(10), 1190-1196. https://doi.org/10.1016/j.cemconres.2008.03.015.

Bogas, J.A. and Nogueira, R. (2014), "Tensile strength of structural expanded clay lightweight concrete subjected to different curing conditions", *KSCE J. Civil Eng.*, **18**(6), 1780-1791. https://doi.org/10.1007/s12205-014-0061-x.

Chen, B. and Fang, C. (2011), "Mechanical properties of EPS lightweight concrete", *Proceedings of the ICE-Construction Materials*, **164**(4), 173-180.

Elzien, A., Ji, B., Fu, Z. and Hu, Z. (2011), "The behavior of lightweight aggregate concrete filled steel tube columns under eccentric loading", *Steel Compos. Struct.*, **11**(6), 469-488. https://doi.org/10.12989/scs.2011.11.6.469.

Haghi, A., Arabani, M. and Ahmadi, H. (2006), "Applications of expanded polystyrene (EPS) beads and polyamide-66 in civil engineering, Part One: Lightweight polymeric concrete", *Compos.Interfaces*, **13**(4-6), 441-450. https://doi.org/10.1163/156855406777408575.

Herki, B. (2017), "Combined effects of densified polystyrene and unprocessed fly ash on concrete engineering properties", *Buildings*, **7**(3), 77. https://doi.org/10.3390/buildings7030077.

Hussin, M., Zhuge, Y., Bullen, F. and Lokuge, W. (2013), "A mathematical model for complete stress-strain curve prediction of permeable concrete", *Proceedings of the 22nd Australasian Conference on the Mechanics of Structures and Materials (ACMSM 22)*, Taylor & Francis (CRC Press)/Balkema.

Kim, D.J., Kim, M.S., Yun, G.Y. and Lee, Y.H. (2013), "Bond strength of steel deformed rebars embedded in artificial lightweight aggregate concrete", *J. Adhesion Sci. Technol.*, **27**(5-6), 490-507.

Lepech, M.D., Li, V.C., Robertson, R.E. and Keoleian, G.A. (2008), "Design of green engineered cementitious composites for improved sustainability", *ACI Mater. J.*, **105**(6), 567-575.

Ling, I. and Teo, D. (2011), "Properties of EPS RHA lightweight concrete bricks under different curing conditions", *Constr. Build. Mater.*, **25**(8), 3648-3655. https://doi.org/10.1016/j.conbuildmat.2011.03.061.

Lo Monte, F., Bamonte, P. and Gambarova, P.G. (2015), "Physical and mechanical properties of heat-damaged structural concrete containing expanded polystyrene syntherized particles", *Fire Mater*., **39**(1), 58-71. https://doi.org/10.1002/fam.2230.

Madandoust, R., Ranjbar, M.M. and Mousavi, S.Y. (2011), "An investigation on the fresh properties of self-compacted lightweight concrete containing expanded polystyrene", *Constr. Building Mater.*, **25**(9), 3721-3731. https://doi.org/10.1016/j.conbuildmat.2011.04.018.

Malvar, L., Cox, J. and Cochran, K.B. (2003), "Bond between carbon fiber reinforced polymer bars and concrete. I: Experimental study", *J. Compos. Constr.*, **7**(2), 154-163. https://doi.org/10.1061/(ASCE)1090-0268(2003)7:2(154).

Miled, K., Sab, K. and Le Roy, R. (2007), "Particle size effect on EPS lightweight concrete compressive strength: experimental investigation and modelling", *Mech. Mater*., **39**(3), 222-240. https://doi.org/10.1016/j.mechmat.2006.05.008.

Park, S.G. and Chisholm, D.H. (1999), "Polystyrene Aggregate Concrete", STUDY REPORT No. 85, Building Research Levy, BRANZ.

Pecce, M., Ceroni, F., Bibbò, F.A. and Acierno, S. (2015), "Steel–concrete bond behaviour of lightweight concrete with expanded polystyrene (EPS)", *Mater. Struct*., **48**(1-2), 139-152. https://doi.org/10.1617/s11527-013-0173-7.

Ranjbar, M.M. and Mousavi, S.Y. (2015), "Strength and durability assessment of self-compacted lightweight concrete containing expanded polystyrene", *Mater. Struct*., **48**(4), 1001-1011. https://doi.org/10.1617/s11527-013-0210-6.

Ravindrarajah, R.S. and Tuck, A. (1994), "Properties of hardened concrete containing treated expanded polystyrene beads", *Cement Concrete Compos*., **16**(4), 273-277. https://doi.org/10.1016/0958-9465(94)90039-6.

RTA-06 (2006), "Materials test methods", Regianl transportation authority , Chichago, IL, USA. 1.

Sabaa, B. and Ravindrarajah, R.S. (1997), "Engineering properties of lightweight concrete containing crushed expanded polystyrene waste. Material Research Society, Fall Meeting Symposium MM, Advances in Materials for Cementitious Composites", Boston, USA.

Sabaa, B. and Ravindrarajah, R.S. (1997), "Engineering properties of lightweight concrete containing crushed expanded polystyrene waste. Materials Research Society, 1997", Fall Meeting, Symposium MM, Advances in Materials for Cementitious Composites December.

Sadrmomtazi, A., Sobhani, J., Mirgozar, M. and Najimi, M. (2012), "Properties of multi-strength grade EPS concrete containing silica fume and rice husk ash", *Constr. Build. Mater.*, **35**, 211-219. https://doi.org/10.1016/j.conbuildmat.2012.02.049.

Schackow, A., Effting, C., Folgueras, M.V., Güths, S. and Mendes, G.A. (2014), "Mechanical and thermal properties of lightweight concretes with vermiculite and EPS using air-entraining agent", *Constr. Build. Mater*., **57**, 190-197. https://doi.org/10.1016/j.conbuildmat.2014.02.009.

Tang, C.W. (2015), "Local bond stress-slip behavior of reinforcing bars embedded in lightweight aggregate concrete", *Comput. Concrete*, **16**(3), 449-466.

Tang, C.W. (2017), "Effect of presoaking degree of lightweight aggregate on the properties of lightweight aggregate concrete", *Comput. Concrete*, **19**(1), 69-78. https://doi.org/10.12989/cac.2017.19.1.069.

Trussoni, M., Hays, C.D. and Zollo, R.F. (2013), "Fracture properties of concrete containing expanded polystyrene aggregate replacement", *ACI Mater. J*., **110**(5).

Vakhshouri, B. and Nejadi, S. (2016), "Mix design of light-weight self-compacting concrete", *Case Studies in Constr. Mater*., **4**, 1-14. https://doi.org/10.1016/j.cscm.2015.10.002.

Vakhshouri, B. and Nejadi, S. (2017). "Review on the mixture design and mechanical properties of the lightweight concrete containing expanded polystyrene beads", *Aus. J. Struct. Eng*., 1-23. https://doi.org/10.1080/13287982.2017.1353330.

Xu, Y., Jiang, L., Xu, J. and Li, Y. (2012), "Mechanical properties of expanded polystyrene lightweight aggregate concrete and brick", *Constr. Build. Mater*., **27**(1), 32-38. https://doi.org/10.1016/j.conbuildmat.2011.08.030.

Yusuf, I. and Jimoh, Y. (2013), "The transfer models of compressive to tensile, flexural and elastic properties of palm kernel shell concrete", *Int. J. Eng. IJE*, **11**(2), 195-200.

CC